Zyxin, a Regulator of Actin Filament Assembly, Targets the Mitotic Apparatus by Interacting with h-warts/LATS1 Tumor Suppressor

Toru Hirota,*‡ Tetsuro Morisaki,* Yasuyuki Nishiyama,* Tomotoshi Marumoto,* Kenji Tada,§ Toshihiro Hara,* Norio Masuko,* Masaki Inagaki,‖ Katsuyoshi Hatakeyama,‡ and Hideyuki Saya*

*Department of Tumor Genetics and Biology, Kumamoto University School of Medicine, 2-2-1 Honjo, Kumamoto 860-0811, Japan; ‡1st Department of Surgery, Niigata University School of Medicine, 1-757 Asahimachi-dori, Niigata 951-8510, Japan; §Department of Neurosurgery, Kumamoto University School of Medicine, 2-2-1 Honjo, Kumamoto 860-0811, Japan; and ‖Laboratory of Biochemistry, Aichi Cancer Center Research Institute, Chikusa-ku, Nagoya, Aichi 464-0021, Japan

Abstract. The mitotic apparatus plays a pivotal role in dividing cells to ensure each daughter cell receives a full set of chromosomes and complement of cytoplasm during mitosis. A human homologue of the *Drosophila* warts tumor suppressor, h-warts/LATS1, is an evolutionarily conserved serine/threonine kinase and a dynamic component of the mitotic apparatus. We have identified an interaction of h-warts/LATS1 with zyxin, a regulator of actin filament assembly. Zyxin is a component of focal adhesion, however, during mitosis a fraction of cytoplasmic-dispersed zyxin becomes associated with h-warts/LATS1 on the mitotic apparatus. We found that zyxin is phosphorylated specifically during mitosis, most likely by Cdc2 kinase, and that the phosphorylation regulates association with h-warts/LATS1. Furthermore, microinjection of truncated h-warts/LATS1 protein, including the zyxin-binding portion, interfered with localization of zyxin to mitotic apparatus, and the duration of mitosis of these injected cells was significantly longer than that of control cells. These findings suggest that h-warts/LATS1 and zyxin play a crucial role in controlling mitosis progression by forming a regulatory complex on mitotic apparatus.

Key words: Cdc2 • interaction • mitotic spindle • phosphorylation • serine/threonine kinase

Introduction

Mitotic apparatus, which consists of a dynamic array of microtubules and associated proteins, controls mitotic events such as establishment of cell polarity, chromosomal congression and segregation, and finally, cytokinesis. Genetic analyses in yeasts and *Drosophila* have identified several kinases essential for normal regulation of mitosis (Glover et al., 1995; Sunkel and Glover, 1988). These mitosis-related serine/threonine kinases have been found to be highly conserved evolutionarily and localized to the mitotic apparatus (Golsteyn et al., 1995; Kimura et al., 1997). Dynamic interaction of these mitosis-related kinases with proteins on the mitotic apparatus is considered to be required to achieve proper coordination of mitotic events (Bahler et al., 1998; Nigg, 1998; Bischoff and Plowman, 1999).

The *warts* gene (also known as *lats*) was identified as a tumor suppressor of *Drosophila melanogaster* (Justice et al., 1995; Xu et al., 1995). The *warts/lats* encodes serine/threonine kinase sharing a high identity with the catalytic domain of myotonic dystrophy protein kinase (DMPK)[1] family, many of which are known to be involved in various mitotic events. Among the DMPK family proteins, *Saccharomyces cerevisiae* Dbf2 was found to be required for completion of mitosis; mutation in *Dbf2* results in a dumbbell-shape phenotype, which is the consequence of cell division failure (Toyn and Johnston, 1994). Orb6, a DMPK homologue in *Schizosaccharomyces pombe*, plays a role in coordinating cell morphogenesis with the cell cycle. Orb6 is known to possess dual functions of both organizing the actin cytoskeleton and negative regulation of mitosis by affecting cdc2 (Verde et al., 1998). The human Rho-associated kinase (Rho kinase) and citron-K kinase, DMPK family members, have been shown to be involved in the regulation of cytokinesis (Madaule et al., 1998; Yasui et al., 1998).

A human homologue of the *warts/lats* gene, termed

Address correspondence to Hideyuki Saya, Department of Tumor Genetics and Biology, Kumamoto University School of Medicine, 2-2-1 Honjo, Kumamoto 860-0811, Japan. Tel.: +81-96-373-5116. Fax: +81-96-373-5120. E-mail: hsaya@gpo.kumamoto-u.ac.jp

[1]*Abbreviations used in this paper:* DMPK, myotonic dystrophy protein kinase; GST, glutathione-*S*-transferase; HA, hemagglutinin 1; KLH, keyhole limpet-hemocyanin; X-gal, 5-bromo-4-chloro-3-indolyl-β-D-galactopyranoside.

h-warts/LATS1, has been identified and demonstrated to negatively regulate Cdc2 activity by interacting with Cdc2 in the mitotic phase (Tao et al., 1999). Analogous to its mutant in *Drosophila*, mice deficient of *LATS1* gene have been shown to develop malignant tumors (St. John et al., 1999). Moreover, h-warts/LATS1 protein was found to localize at the centrosome in interphase and to translocate dynamically toward mitotic spindles in metaphase-anaphase, and, finally, to the midbody by telophase (Nishiyama et al., 1999). Recently, the Sid2 kinase, structural homologue of Dbf2 and a potential counterpart of h-warts/LATS1 in fission yeast, has been demonstrated to function as part of a novel signaling pathway required for onset of cytokinesis. Sid2 is a component of the spindle pole body and by virtue of its transient localization to the division site, it appears to determine the timing of ring constriction (Sparks et al., 1999). Based on these observations, h-warts/LATS1 is speculated to be heavily involved in mitotic events in mammalian cells and that loss of its function disrupts normal cell cycle regulation, leading to the development of tumors. Therefore, identification of cellular targets of the h-warts/LATS1 protein will provide clues to its precise cell cycle function and to its involvement in tumorigenesis.

During mitosis, adherent cells change morphology into a spheroid and weakly adherent form. This morphological alteration involves rearrangement of cytoskeletal systems and dissociation of the adhesion apparatus, which are under the control of biochemical status through cell cycle progression (Verde et al., 1998). Focal adhesion plaques are an adhesion apparatus for cells to contact the extracellular matrix where the growing end of actin filament attaches to the plasma membrane. At the focal adhesion complex, a number of proteins serve as linkages between transmembrane proteins and the actin cytoskeleton, regulating actin filament dynamics (Craig and Johnson, 1996; Beckerle, 1997). As cells proceed through mitosis, components of the focal adhesion complex are known to dissociate into the cytoplasm when bundles of actin fibers disappear. The role of these actin-regulatory proteins during mitosis, which are dispersed in the cytoplasm, remains to be established.

Zyxin is a component of the focal adhesion complex (Crawford and Beckerle, 1991) and plays a central role in actin filament polymerization in mammalian cells (reviewed in Beckerle, 1997). Several lines of evidence demonstrate that zyxin may function to recruit components required for the actin assembly machinery to specific sites in the cell and to stimulate spatially restricted actin polymerization (Crawford et al., 1992; Reinhard et al., 1995; Hobert et al., 1996; Prehoda et al., 1999). Interestingly, zyxin exhibits a functional nuclear export signal and has been demonstrated to shuttle between the nucleus and the sites of cell adhesion (Nix and Beckerle, 1997). These findings suggest that zyxin has an unknown second function in addition to its key role in regulating actin assembly.

In this study, we have identified the interaction of h-warts/LATS1 with zyxin on the mitotic apparatus during mitosis. The localization of zyxin on the mitotic apparatus appears to be dependent on the presence of h-warts/LATS1 protein. Furthermore, we showed that zyxin is phosphorylated specifically during mitosis, most likely by Cdc2 kinase, and that this phosphorylation controls the association of zyxin with h-warts/LATS1. The interaction between zyxin and h-warts/LATS1 on the mitotic apparatus implicates a significant role for actin regulatory proteins during mitosis.

Materials and Methods

Yeast Two-Hybrid Screening

Yeast strain L40 was used as a host for the two-hybrid screening (Vojtek et al., 1993). An L40 strain carrying pBTM116HA/h-warts (amino acids 394–675) was transformed with the HeLa cDNA library constructed in pGAD-GH (Clontech) by electroporation. Transformants were screened for growth on SD plate media lacking tryptophan, leucine, and histidine prototrophy. His^+ colonies were subjected to β-galactosidase assay. Plasmids harboring cDNA were recovered from positive colonies and the nucleotide sequence of plasmid DNA which conferred the $LacZ^+$ phenotype on L40 containing pBTM116HA/h-warts (396–657) were determined.

Cell Culture, Synchronization, and Transfections

HeLa, COS7, and U2OS cells were cultured in DME/F12 supplemented with 10% fetal calf serum without antibiotics. HeLa cells were synchronized at the beginning of S phase by double thymidine block and release protocol (first 24 h incubation with 1 mM thymidine, an interval of thymidine-free incubation for 8 h, and second thymidine incubation for 14 h). Mitotic cells were collected by mechanical shake-off from the culture plate 9.5 h after release from S phase. For transient transfection, cells in 6-well plates were transfected using FuGene6 transfection reagent following the manufacturer's instructions (Boehringer Mannheim). To prepare for flow cytometry, cells were trypsinized, fixed with 70% methanol, and DNA were stained with propidium iodide. Cells were subjected to flow cytometry on FACScan® (Becton Dickinson). G1, S, and G2/M populations were calculated with ModFit 2.1 software (Varity).

Expression Plasmids

Mammalian expression plasmids were constructed by subcloning the PCR amplified fragment into hemagglutinin 1 (HA)-tagged (pCGN), FLAG-tagged (pBJ-FLAG) vectors. pBJ-FLAG, was constructed by inserting an annealed oligonucleotide between the XhoI and BamHI sites of pBJ-myc. All the PCR products were obtained using PyroBest DNA polymerase (Takara) and we confirmed their sequences. For glutathione-*S*-transferase (GST) fusion protein expression in bacteria, pGEX2TH-based plasmids were constructed as previously described (Masuko et al., 1999).

Antibody Preparation

Two polyclonal antibodies against h-warts/LATS1 were generated by injecting rabbits with two synthetic peptides, C1 (PVDPDKLWSDDNEEENVNDTLNG), and C2 (SDEDDQNTGSEIKNRDLVYV), coupled to keyhole limpet-hemocyanin (KLH) via the added NH_2-terminal cysteine. GST–h-warts amino acids 136–700 and amino acids 136–410 were also used for immunizing rats, generating G3 and G4 antisera, respectively. The polyclonal antibody against zyxin was generated in rabbit as previously described (Macalma et al., 1996), or purchased from Santa Cruz. Monoclonal antibodies for HA-epitope (12CA5) and FLAG-epitope (M5) were obtained from Boehringer Mannheim and Sigma-Aldrich, respectively. Monoclonal antibodies for α-tubulin (clone B512), vinculin and cyclin B were purchased from Sigma-Aldrich and Transduction Laboratories, respectively.

Immunoprecipitation

Cells were lysed on ice for 30 min with 0.5% NP-40 lysis buffer consisting of 0.5% NP-40, 25 mM Tris-Cl, pH 7.5, 137 mM NaCl, 1 mM EDTA, 1 mM EGTA, 5% glycerol, 2 μg/ml aprotinin, 20 mM β-glycerophosphate, 1 mM ABSF, 10 μM leupeptin, 1 μM pepstatin, and 1 mM Na_3VO_4. Lysates were centrifuged at 14,000 *g* for 20 min. Aliquots of supernatant (200 μg, ~2.0 mg/ml) were incubated for 1 h at 4°C with specific antibodies, and another 1 h incubation after adding 30 μl of protein G/A agarose beads (50% slurry; Calbiochem). After being washed, the bound proteins were analyzed by immunoblotting.

For coimmunoprecipitation of h-warts/LATS1 and zyxin, HeLa cells were lysed on ice for 30 min with five cell volumes of the 0.1% NP-40 lysis buffer (0.1% NP-40, 100 mM NaCl, 25 mM Tris-Cl, pH 8.0, 5 mM EGTA, 1 mM $MgCl_2$ and 5% glycerol supplemented with 1 mM DTT, 2 μg/ml aprotinin, 20 mM β-glycerophosphate, 1 mM ABSF, 10 μM leupeptin, 1 μM pepstatin, 1 mM Na_3VO_4, 1 mM benzamidine, and 1 μM microcystin), and centrifuged at 14,000 *g* for 20 min. Precleared 400 μg quantities of cell lysate (~4 mg/ml) were mixed with 3 μl of anti-zyxin antibody for 3 h on ice, then 15 μl of protein A–Sepharose beads (Amersham Pharmacia) were added and incubated for another 2 h at 4°C. After washing five times with the 0.1% NP-40 lysis buffer, the lysate was eluted by boiling for 3 min in 62.5 mM Tris-Cl, pH 6.8, containing 2% SDS and 10% glycerol. The elute was removed, made to 10 mM DTT and 0.1% bromophenol blue, boiled again and then subjected to immunoblotting. Quantification analysis was performed by MacBAS v2.5 software.

In Vitro Pull-Down Assay and Solution-Binding Assay

For pull-down assay, 30 μg of GST fusion protein was immobilized on glutathione-agarose, and equilibrated with 0.5% NP-40 lysis buffer. Aliquots of cell lysate (200 μg, ~2.0 mg/ml) were incubated with the glutathione-agarose for 1 h. The bound proteins were analyzed by immunoblotting. In vitro solution binding assay was performed as described (Jin et al., 1998). In brief, 10 μg of GST fusion proteins was immobilized on the glutathione-agarose and equilibrated with buffer B (20 mM Hepes-KOH, pH 7.9, 50 mM NaCl, 1 mM $MgCl_2$, 17% glycerol, and 2 mM DTT). The glutathione-agarose were incubated with 1 μg of His-h-warts in 200 μl of buffer B for 1 h at 4°C. After extensive washing with buffer B, the bound proteins were analyzed by immunoblotting.

In Vitro Kinase Assay

Synchronized HeLa cells were washed with ice-cold PBS and lysed on the plate with RIPA buffer as previously described (Izawa et al., 1996). Lysates were centrifuged at 14,000 *g* for 20 min, and the supernatant was used for the kinase assays. Kinase reaction were conducted at 25°C for 30 min in a final volume of 50 μl containing 20 mM Tris, pH 7.4, 10 mM $MgCl_2$, 10 μCi of γ-[^{32}P]ATP (3,000 Ci/mmol; Amersham Pharmacia), 1 μM microcystin, 8 μg of cell lysates, and 10 μg of GST-zyxin. Each reaction mixture was then chilled and mixed with 30 μl of glutathione-agarose beads (50% slurry) and 0.5 ml of ice-cold TNE buffer, followed by rocking for 30 min at 4°C. The glutathione-agarose beads were washed and boiled in 30 μl of Laemmli sample buffer to elute GST fusion proteins. The samples were resolved by 8% SDS-PAGE and visualized by autoradiography. The result of gel analyses were quantified by MacBAS (Fujifilm).

Depletion of Cdc2

Aliquots of 150 μl of mitotic cell lysate (1.0 mg/ml) were incubated with 50 μl of p13-suc1 agarose beads (50% slurry; Upstate Biotechnology) at 4°C for 45 min. After centrifugation, 50 μl of fresh p13 suc1-beads was added to the supernatant and incubated for an additional 30 min. The Cdc2 kinase assay was performed by the SignaTECT assay system (Promega) in which biotinylated peptide derived from histone H1 was used as a substrate and radiolabeled phosphorylated substrate was recovered with streptoavidin matrix. The purified active Cdc2 kinase was prepared as previously described (Kusubata et al., 1992).

Immunofluorescence Microscopy

U2OS cells were grown on a 35-mm petri dish to ~70% confluence, fixed with 4% paraformaldehyde/PBS, pH 7.4, for 15 min at room temperature, followed by permeabilization with 0.2% Triton X-100/PBS, otherwise fixed with a methanol/acetone solution for 10 min on ice. A preextraction protocol was performed either with 7.5 μg/ml digitonin in KHM buffer (25 mM Hepes-KOH, pH 7.2, 125 mM potassium acetate, 2.5 mM magnesium acetate) or with microtubule stabilizing buffer (MSB; 80 mM Pipes-KOH, pH 6.8, 5 mM EGTA, 1 mM $MgCl_2$ containing 0.5% Triton X-100) for 5 min at room temperature before fixing with chilled absolute methanol for 10 min at −20°C as described (Terada et al., 1998). After being washed, cells were incubated with the following antibodies: rabbit anti-zyxin antibody, rat anti–h-warts antibody (G3), and monoclonal mouse anti–α-tubulin antibody (B512). This was followed by incubation with FITC-conjugated anti–rabbit/mouse IgG antibody (Amersham Pharmacia), Cy3-conjugated anti-rat IgG antibody (Amersham Pharmacia), and Texas red–conjugated anti-mouse IgG antibody (Molecular Probes). The stained cells were mounted with 1,4-diazabicyclo-[2,2,2]-octane/glycerol, and observed with confocal microscopy (Fluoview; Olympus). Images were obtained separately by independent excitation at 488/568 nm to minimize overlapping signals, and were processed using Photoshop software (Adobe).

Microinjection

U2OS cells were grown on 35-mm petri dishes to 75% confluency and microinjected using semi-automatic micro-manipulator/injector (Eppendorf 5171/5246). Cells in prometaphase were selected for injection on the basis of morphology by phase contrast images, and injected with a 1.0 mg/ml solution of purified GST fusion proteins and rhodamine-tubulin (Cytoskeleton) in PBS, pH 6.9, supplemented with a final concentration of 0.5 mM GTP. The microscopical stage was maintained at 37°C and the procedure was completed within 20 min to minimize pH changes. After injection, cells were incubated at 37°C for 20 min for rhodamine-tubulin to be distributed to the mitotic spindle, followed by detergent preextraction (7.5 μg/ml digitonin in KHM buffer) and a methanol fixation protocol as described above.

Synchronized HeLa cells were injected into the cytoplasm with a combination of 1.0 mg/ml solution of purified GST fusion proteins together with 1.0 mg/ml β-galactosidase (Sigma-Aldrich). Cells were fixed with 0.5% glutaraldehyde/PBS, pH 7.2, at subsequent time points, followed by incubation with 1 mg/ml of 5-bromo-4-chloro-3-indolyl-β-D-galactopyranoside (X-gal) in 150 mM NaCl, 0.01% sodium deoxycholate, 0.02% NP-40, 2 mM $MgCl_2$, 5 mM $K_3Fe(CN)_6$, and 5 mM $K_4Fe(CN)_6$ for 12 h at 37°C. After removing the X-gal solution, cells were overlaid with acreto-orcein (Merck) in 60% acetic acid to visualize chromatin.

Results

Identification of h-warts/LATS1 Interacting Protein

To identify proteins that physically interact with h-warts/LATS1, we conducted a HeLa cDNA library screen by the yeast two-hybrid method. We used a region of amino acids 394–675, which does not contain the kinase domain of h-warts/LATS1, as the bait for the screen (Fig. 1 A). From 2.3×10^6 initial transformants, 53 clones were found to confer both the His^+ and $LacZ^+$ phenotypes on L40 containing pBTM116HA/h-warts. These positive clones were subjected to secondary screening to eliminate false positives, and confirmed the specific interaction between h-warts/LATS1 and protein encoded by a library cDNA within the yeast cells. Among the positive clones, we isolated four independent cDNA clones encoding partial protein fragments that derived from zyxin, a regulator of actin assembly (Fig. 1 A). The other h-warts/LATS1-interacting proteins identified in this screen will be described elsewhere.

Interaction of Zyxin with h-warts/LATS1

To examine whether zyxin interacts with h-warts/LATS1 in intact cells, we coexpressed zyxin with h-warts/LATS1 in COS7 cells (Fig. 1 B). Full-length zyxin and full-length h-warts/LATS1 were tagged with FLAG and HA epitopes, respectively, at their NH_2 termini. When the lysate coexpressing FLAG-zyxin with HA-h-warts/LATS1 was immunoprecipitated with the anti-FLAG antibody, HA-h-warts/LATS1 was detected in the FLAG-zyxin immune complex (Fig. 1 C, lane 1). Conversely, FLAG-zyxin was detected in the HA-h-warts/LATS1 immune complex (Fig. 1 C, lane 4). Neither FLAG-zyxin nor HA-h-warts/LATS1 was detected in the unrelated control IgG immunoprecipitates from lysates expressing both proteins (data not shown).

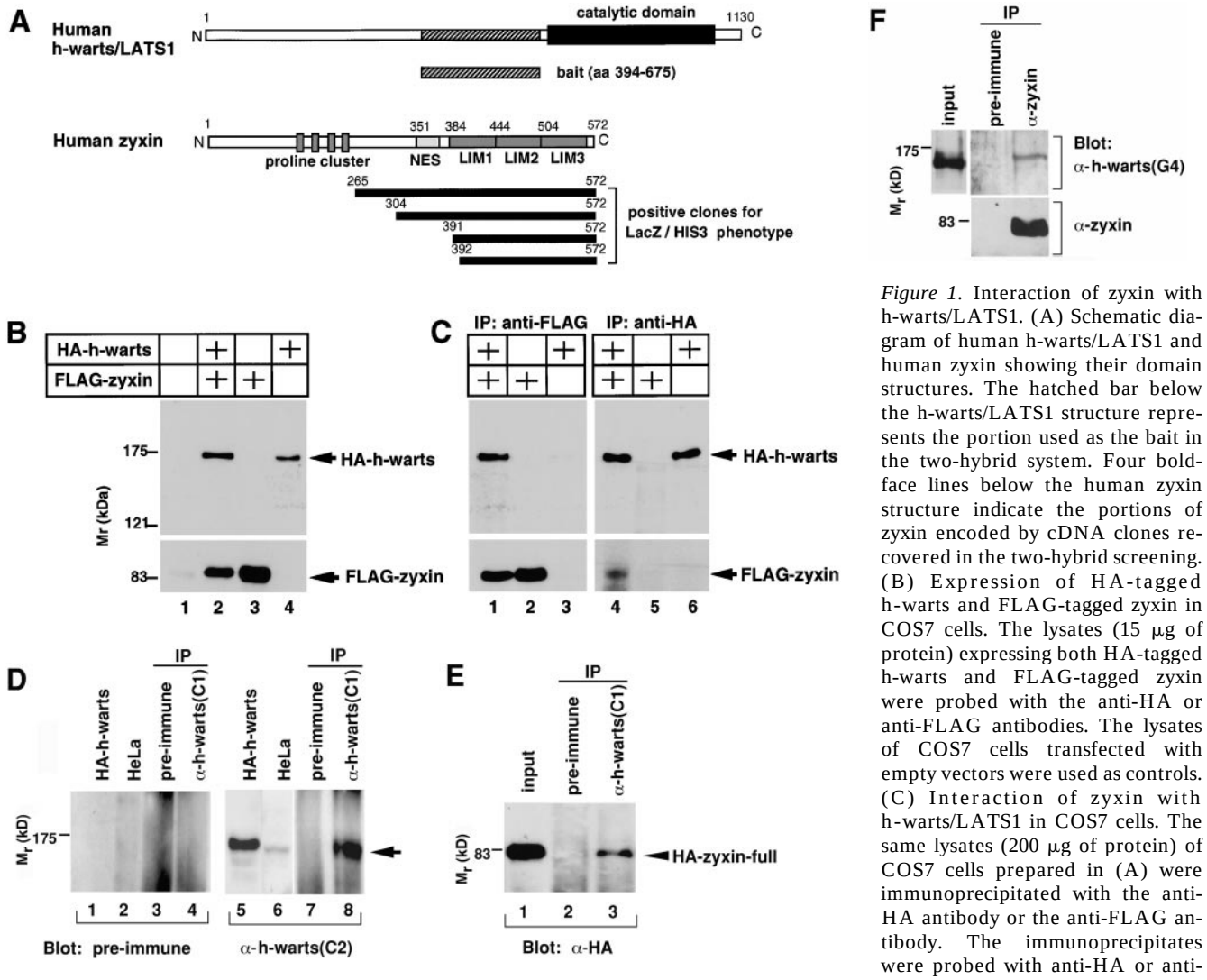

Figure 1. Interaction of zyxin with h-warts/LATS1. (A) Schematic diagram of human h-warts/LATS1 and human zyxin showing their domain structures. The hatched bar below the h-warts/LATS1 structure represents the portion used as the bait in the two-hybrid system. Four boldface lines below the human zyxin structure indicate the portions of zyxin encoded by cDNA clones recovered in the two-hybrid screening. (B) Expression of HA-tagged h-warts and FLAG-tagged zyxin in COS7 cells. The lysates (15 μg of protein) expressing both HA-tagged h-warts and FLAG-tagged zyxin were probed with the anti-HA or anti-FLAG antibodies. The lysates of COS7 cells transfected with empty vectors were used as controls. (C) Interaction of zyxin with h-warts/LATS1 in COS7 cells. The same lysates (200 μg of protein) of COS7 cells prepared in (A) were immunoprecipitated with the anti-HA antibody or the anti-FLAG antibody. The immunoprecipitates were probed with anti-HA or anti-zyxin antibodies. (D) Specificity of the h-warts/LATS1 antibody. Lysates of COS7 cells expressing HA-tagged h-warts (lanes 1 and 5), HeLa cell lysate (lane 2), and HeLa cell lysate immunoprecipitated with preimmune IgG (lanes 3 and 7) or with the anti-C1 antibody (lanes 4 and 8) were immunoblotted by preimmune IgG (lanes 1–4) or by the anti-C2 antibody (lanes 5–8). Arrow indicates endogenous h-warts/LATS1. (E) Endogenous h-warts/LATS1 interacts with zyxin. The lysate of COS7 cells expressing HA-tagged zyxin (full-length) was immunoprecipitated with the anti-C1 antibody (lane 3), or with preimmune IgG (lane 2). The immunoprecipitates were probed with the anti-HA antibody. (F) Coimmunoprecipitation of endogenous h-warts/LATS1 and zyxin. The lysate of HeLa cells was immunoprecipitated with preimmune IgG or with the anti-zyxin antibody generated in rabbits as described in Fig. 3. Equal amount of cell lysate was immunoprecipitated with anti–h-warts/LATS1 antibody to quantify the endogenous protein in the aliquot of lysate (input). The immunoprecipitates were probed with the rat anti–h-warts/LATS1(G4) antibody (upper), and the goat anti-zyxin antibody (lower), as indicated.

An additional experiment to confirm the interaction of zyxin with h-warts/LATS1 was performed. Two polyclonal antibodies were raised against h-warts/LATS1 by injecting two KLH-conjugated synthetic polypeptides, C1 (amino acids 1,041–1,063) and C2 (amino acids 1,111–1,130), into rabbits. Endogenous h-warts/LATS1 was immunoprecipitated by the anti-C1 antibody and was detected at immunoblotting by the anti-C2 antibody (Fig. 1 D, lane 8). When the COS7 cell lysate expressing HA-tagged zyxin (full-length) was immunoprecipitated with the anti-C1 antibody, HA-zyxin (full-length) was coprecipitated with endogenous h-warts/LATS1 (Fig. 1 E, lane 3).

Furthermore, we tested whether endogenous zyxin and h-warts/LATS1 interact in vivo. Using anti-zyxin antibody generated in rabbits, zyxin was immunoprecipitated from HeLa cell lysate. The endogenous h-warts/LATS1 was detected in the immunoprecipitate (Fig 1 F). Although comparison of the band profiles revealed that the small fraction of h-warts/LATS1 (~9%) interacts with zyxin, these results indicate the association of h-warts/LATS1 and zyxin in intact cells.

Since zyxin harbors three copies of LIM domain in the COOH-terminal third of the molecule (Fig. 2 A), known as a protein–protein interacting structure, we first examined whether the LIM domain of zyxin serves as a binding interface for h-warts/LATS1 interaction. COS7 cell lysates

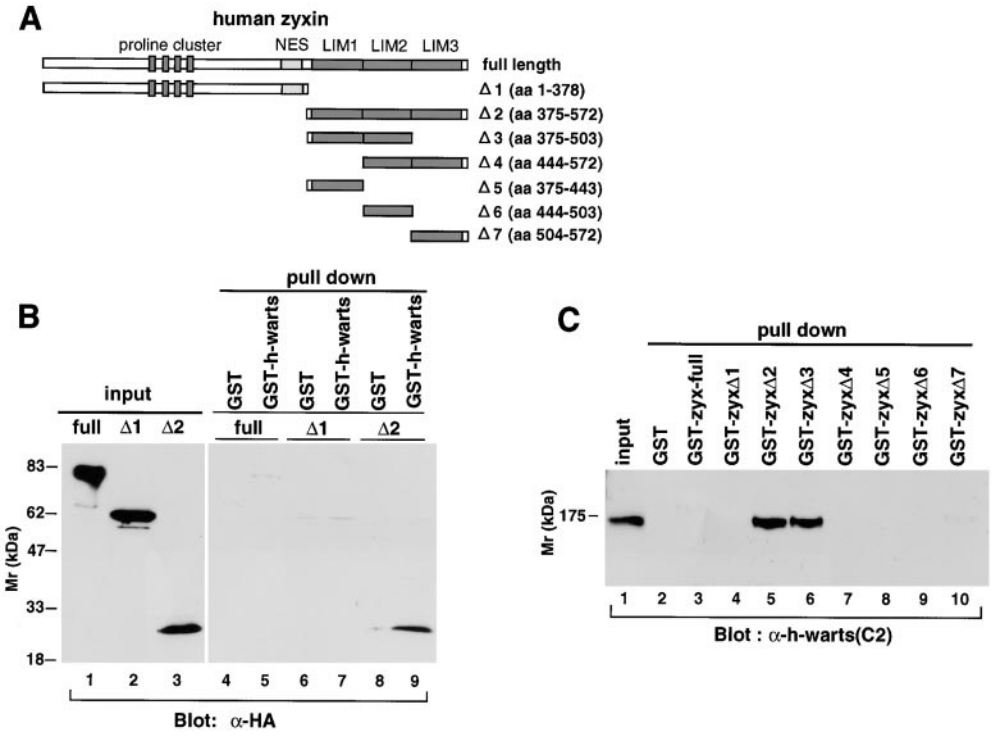

Figure 2. In vitro interaction of h-warts/LATS1 and zyxin. (A) Schematic diagram of deletion mutant zyxin showing their domain structures. The NH_2-terminal two-thirds mutant (Δ1) contains four copies of a proline rich cluster and the nuclear exporting signal (NES), and the COOH-terminal third mutant (Δ2) contains three copies of the LIM domain. LIM domains were constructed tandemly or independently as indicated (Δ3–Δ7). The HA-tag epitope or the GST region of the fusion protein is not shown. (B) The lysates of COS7 cells expressing the indicated HA-tagged zyxin full-length and mutants (lanes 1–3) were subjected to incubation with either GST alone (lanes 4, 6, and 8) or GST–h-warts/LATS1 (amino acids 136–700) resin (lanes 5, 7, and 9). The bound fraction was analyzed by SDS-PAGE, followed by immunoblotting with anti-HA antibody. (C) In vitro binding assay between recombinant h-warts/LATS1 and zyxin. 10 μg of the purified GST-zyxin deletion mutants, as shown in (A), were immobilized to resins, and incubated with purified His-tagged h-warts/LATS1 (1.0 μg of protein) generated in baculovirus-infected Sf9 cells. The bound fraction was analyzed by immunoblotting with the anti-C2 antibody.

expressing HA-tagged zyxin either full-length, NH_2-terminal two-thirds (Δ1) or COOH-terminal third (Δ2), which contains three LIM domains, were incubated with GST–h-warts/LATS1 (amino acids 136–700) fusion protein bound to glutathione-agarose beads (Fig. 2 B, lanes 1–3). The pull-down assay revealed that HA-zyxinΔ2 coprecipitated with GST–h-warts/LATS1 but HA-zyxinΔ1 did not (Fig. 2 B, lanes 7 and 9). Unexpectedly, the full-length HA-zyxin was hardly detectable in the GST–h-warts precipitate (Fig. 2 B, lane 5).

We next sought to delineate in detail the region(s) of zyxin important for its association with h-warts/LATS1 using GST fusion proteins containing a full-length or various truncated zyxin (Fig. 2 A). Same amounts of GST-zyxin fusion proteins bound to glutathione-agarose beads were incubated with baculoviral expressed His-tagged h-warts (full-length), and the retained proteins were analyzed by immunoblotting with anti-C2 antibody. While GST-zyxin-LIM1/2 (Δ3) and GST-zyxin-LIM1/2/3 (Δ2) were found to bind with purified h-warts protein, the other GST-zyxin mutants did not (Fig. 2 C). This in vitro binding experiment demonstrated that zyxin directly interacts with h-warts/LATS1 and that the region containing both LIM1 and LIM2 domains of zyxin is essential for their binding.

Interestingly, consistent with the findings shown in Fig. 2 A, GST-zyxin (full-length) did not interact with His-tagged h-warts/LATS1. However, their association was detected in in vivo binding assays (Fig. 1, C, E, and F). Based on these findings, we speculated that the LIM1/2 domains are masked in full-length zyxin and that an intramolecular and/or intermolecular modification may regulate the interaction between zyxin and h-warts/LATS1.

Localization of h-warts/LATS1–Zyxin Complex to Mitotic Apparatus

Next, we compared the subcellular localization of h-warts/LATS1 and zyxin by immunocytochemical analysis. We raised antibody against zyxin (amino acids 24–35) in rabbits by the procedure described by Macalma et al. (1996). Consistent with their previous characterization, this antibody recognized a single band of ~82 kD, which is described as the molecular mass of full-length zyxin by immunoblotting (Fig. 3 A). Indirect immunofluorescent studies revealed that the antibody specifically detected concentrated zyxin at the focal adhesion plaques, where the bundles of actin filaments end (Fig. 3 B). In the mitotic cells, the characteristic staining of zyxin was found to disappear from focal adhesions and was seen as a diffuse cytoplasmic distribution (Fig. 3 C). A similar change in subcellular distribution was observed in vinculin, another focal adhesion protein with a proline-rich stretch functionally related to zyxin, as cells retracted and rounded up during mitosis (data not shown). Notably, with careful observation of the zyxin immunostaining, a zyxin signal was barely seen at the mitotic apparatus (Fig. 3 C, b, arrows). This signal became more distinct when cells were fixed with acetone/methanol solution (Fig. 3 D).

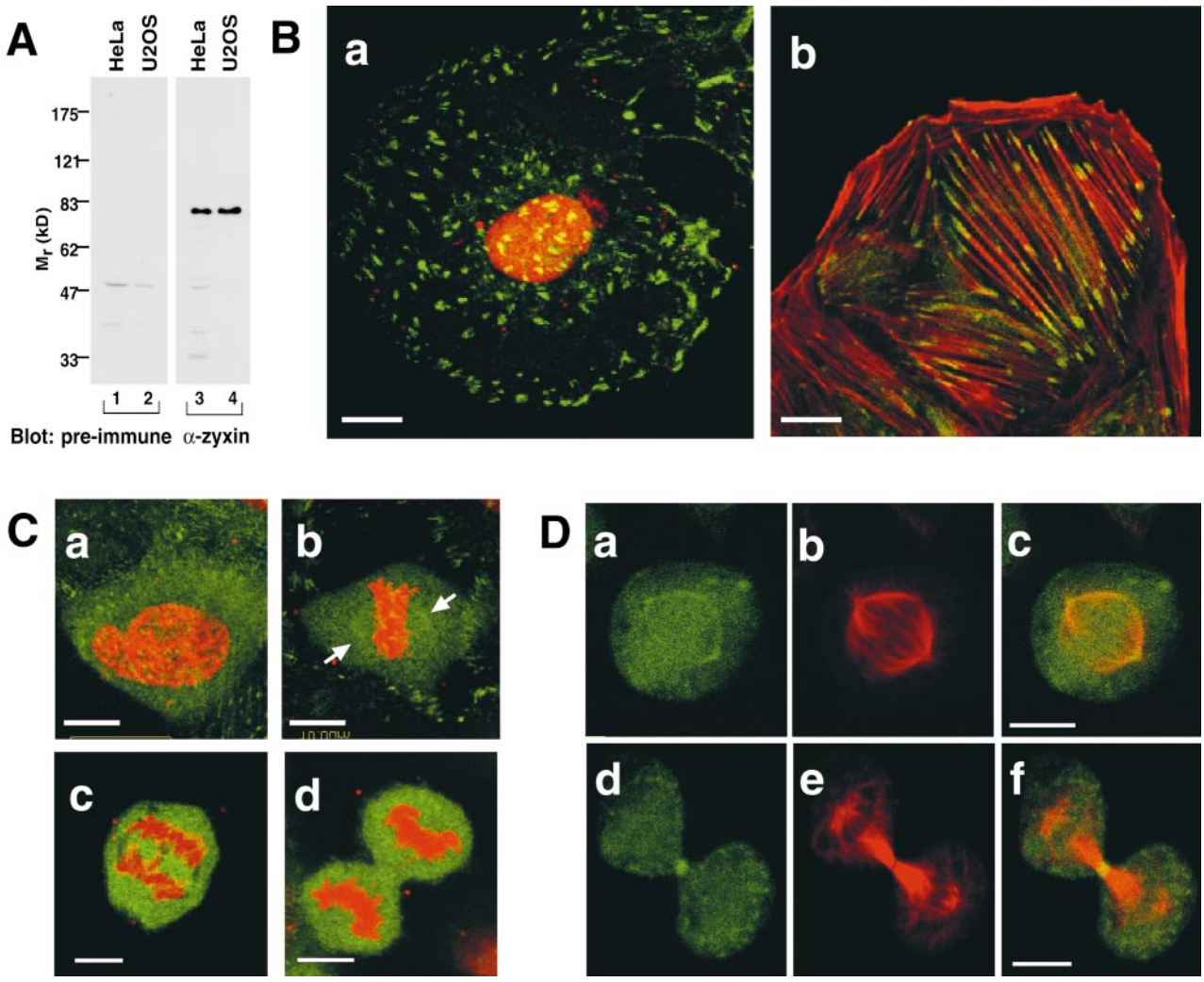

Figure 3. Specificity of the anti-zyxin antibody. (A) Total lysates of HeLa cells (lanes 1 and 3), and U2OS cells (lanes 2 and 4) were resolved in 12% SDS-PAGE, followed by immunoblotting with either the preimmune IgG (lanes 1 and 2) or the anti-zyxin antibody (lanes 3 and 4). (B) Subcellular localization of endogenous zyxin. Subconfluently grown U2OS cells were fixed with 4% paraformaldehyde and processed for indirect immunofluorescent staining with the anti-zyxin antibody labeled by FITC. DNA was visualized by propidium iodide (a), and F-actin by rhodamine-phalloidin (b). (C) Distribution of zyxin during the cell cycle. U2OS cells were prepared as in (B, a). Representative cells in prophase (a), metaphase (b), anaphase (c), and telophase (d) are shown. (D) Detection of zyxin on the mitotic apparatus. U2OS cells were fixed with acetone/methanol solution and processed for immunostaining with the anti-zyxin antibody labeled with FITC (a and d) and anti-tubulin antibody labeled with Cy3 (b and e). The merged picture of the left two panels are shown in the right panel (c and f). Representative cells in metaphase (a–c) and telophase (d–f) are shown. Bars, 10 μm.

To examine localization in detail, cells were processed in a detergent-preextraction protocol which washes out the free cytoplasmic proteins. As previously reported, h-warts/LATS1 locates to centrosomes during interphase (Fig. 4 A, a–c). When cells enter prometaphase/metaphase, h-warts/LATS1 translocates toward the mitotic spindle array as well as the spindle poles (Fig. 4 A, d–f). As the cell commits to anaphase (Fig. 4 A, g–i) and later to telophase (Fig. 4 A, j–l), h-warts/LATS1 is found progressively at the bundle of microtubules at the midzone, called the central spindle, that connects daughter cells (Fig. 4 A, m–o). The detergent-preextraction immunostaining procedure showed that a fraction of zyxin was also found to associate with mitotic apparatus during mitosis. As cells entered mitosis, when assembly of the mitotic spindle begins from spindle poles, zyxin initially located to the mitotic spindle (Fig. 4 B, a–c), and this association with the mitotic spindle became prominent by metaphase (Fig. 4 B, d–f). As cells proceeded into anaphase, zyxin was detected on the spindle between segregated sister chromatids, which are composed of bidirectional overlapping polar spindle (Fig. 4 B, g–i). In late anaphase, zyxin became detectable as a distinct wide band extending across the midzone of the central spindle (Fig. 4 B, j–l). This central spindle staining persisted into telophase when the spindle compacts into the midbody (Fig. 4 B, m–o). These specific staining patterns on the mitotic apparatus were neither detected with the preimmune IgG nor with anti-vinculin antibody (data not shown). When cells were double-stained for h-warts/LATS1 and zyxin, the yellow color produced by superim-

posing green and red demonstrated that h-warts/LATS1 and zyxin colocalize on the mitotic spindle, spindle poles and midbody of the dividing cells (Fig. 4 C). The dynamic changes in zyxin and h-warts/LATS1 localization on the mitotic apparatus is identical, suggesting that zyxin interacts with h-warts/LATS1 on the mitotic apparatus, including mitotic spindle and central spindle at midzone of the dividing cells.

Specific Phosphorylation of Zyxin during Mitosis

Since h-warts/LATS1 was reported to be posttranslationally modified in a cell cycle–specific manner and to play a critical role in cell cycle regulation (Tao et al., 1999; Nishiyama et al., 1999), we asked whether zyxin also has any cell cycle phase-specific changes concomitant with that of h-warts/LATS1 protein. For cell cycle analysis, HeLa cells were synchronized at the beginning of S phase by double thymidine block method. At different times after release from block, cells were harvested and analyzed for zyxin by immunoblotting with anti-zyxin antibody (Fig. 5 A). Although levels of zyxin expression did not change throughout the cell cycle, a slow-migrating form of zyxin appeared in cells at 9 and 10 h after release from S phase, where considerable number of cells were in the mitotic phase as monitored by cyclin B protein level (Fig. 5 A, lanes 4 and 5). This slow migrating band became prominent when cells were treated with the microtubule-depolymerizing agent, nocodazole (Fig. 5 A, lane 8), whereas vinculin protein remained stable throughout cell cycle. To test whether this mitosis-specific modification of zyxin is phosphorylation, we examined the effect of phosphatase treatment on the mobility shift. The slow-migrating bands found in the mitotic and nocodazole-treated cell lysates were converted into the fast-migrating bands after zyxin was incubated with calf intestine alkaline phosphatase (Fig. 5 B, lanes 4 and 6). These results indicate that the slow-migrating form is phosphorylated zyxin, and that zyxin is specifically phosphorylated during mitosis.

For an additional approach to demonstrate the specific phosphorylation of zyxin during mitosis, in vitro kinase assay using cell lysates was employed. We used cell lysates from various phases in the cell cycle as sources of the enzyme and GST-zyxin as the substrate. GST-zyxin was phosphorylated significantly with mitotic cell lysate (Fig. 5 C, lane 3). To determine the phosphorylation region(s) in the molecule GST-zyxinΔ1 and GST-zyxinΔ2 were processed for the in vitro kinase assay. GST-zyxinΔ1, which corresponds to the NH_2-terminal two thirds of zyxin, was significantly phosphorylated with mitotic cell lysate whereas no phosphorylation was detected in GST-zyxinΔ2 (Fig. 5 D).

Characterization of Zyxin-Kinase during Mitosis

To address the class to which zyxin-kinase belongs, we used various specific inhibitors that have been developed for kinases. The kinase assay was performed with mitotic cell lysates which were preincubated with various kinase inhibitors (Fig 6 A). GST-zyxin phosphorylation activity in the cell lysate was specifically inhibited not only when the mitotic cell lysate was preincubated with the broad serine/threonine kinase inhibitor staurosporine (100 nM), but also after preincubation with olomoucine, which is a specific inhibitor of Cdc2 (Fig. 6 A). Therefore, to examine whether Cdc2 kinase is the responsible kinase for zyxin phosphorylation in the mitotic cell lysate, we prepared mitotic cell lysate depleted of Cdc2, which should contain the full complement of mitotically active kinases except for Cdc2, including kinases activated downstream of Cdc2 (Fig. 6 B). By monitoring the total protein concentration and the Cdc2 kinase activity of the depleted mitotic cell lysate (Fig. 6 C), we found that phosphorylation of GST-zyxin was significantly inhibited by depleting Cdc2 from the mitotic cell lysate (Fig. 6 D, lane 3). Addition of active Cdc2 complex to the Cdc2-depleted mitotic cell lysate restored the phosphorylation activity (Fig. 6 D, lane 4), indicating that loss of zyxin phosphorylating activity was due to removal of Cdc2 but not to other components in the lysate. Furthermore, the purified Cdc2 kinase complex was sufficient for zyxin phosphorylation without requiring any other components (Fig. 6 E). These data demonstrate that Cdc2 is a kinase responsible for the mitosis-specific phosphorylation of zyxin in vitro, even though other active kinases are present in the mitotic lysate.

Phosphorylation of Zyxin by Cdc2 Regulates Binding to h-warts/LATS1

Three lines of evidence suggest that zyxin interacts with h-warts/LATS1 during mitosis and that the interaction is regulated by the phosphorylation of zyxin. First, zyxin undergoes posttranslational modification during mitosis, which was shown to be phosphorylation. Second, h-warts/LATS1 binds to the region containing LIM1 and LIM2 domains of zyxin and an intra/inter-molecular modification of zyxin may be required for h-warts/LATS1 to access to the binding domains. Third, a fraction of zyxin is distributed to the mitotic apparatus, where it colocalizes with h-warts/LATS1 protein. Since our results demonstrated that Cdc2 is the kinase responsible for mitotic phosphorylation of zyxin, we postulated that the Cdc2-mediated phosphorylation of zyxin promotes interaction between zyxin and h-warts/LATS1. To test this possibility, GST-zyxin (full-length) was phosphorylated by active Cdc2 complex, followed by incubation with recombinant His-tagged h-warts/LATS1. His-tagged h-warts/LATS1 precipitated with phosphorylated GST-zyxin (Fig. 7 A, lane 5) while the control unphosphorylated GST-zyxin did not (Fig. 7 A, lanes 2 and 4).

Furthermore, to examine whether zyxin associates with h-warts/LATS1 specifically during mitosis in the intact cells, endogenous zyxin was immunoprecipitated from either interphase or mitotic cell lysate and probed with anti–h-warts/LATS1 antibody. The endogenous h-warts/LATS1 coprecipitated with zyxin from mitotic lysate was found to be more abundant than that from interphase cell lysate (Fig. 7 B, lane 4). These results indicates that zyxin interacts with h-warts/LATS1 during mitosis, and that the interaction is regulated by phosphorylation of zyxin. This mitosis-specific interaction explains why the proportion of the zyxin-binding h-warts/LATS1 to its entire pool was less than 10% in asynchronized cells (Fig. 1 F). It is also interesting to note that the zyxin-binding h-warts/LATS1 migrated slower than its entire pool (Fig. 1 F), suggesting that mitotic phosphorylated form of h-warts/LATS1

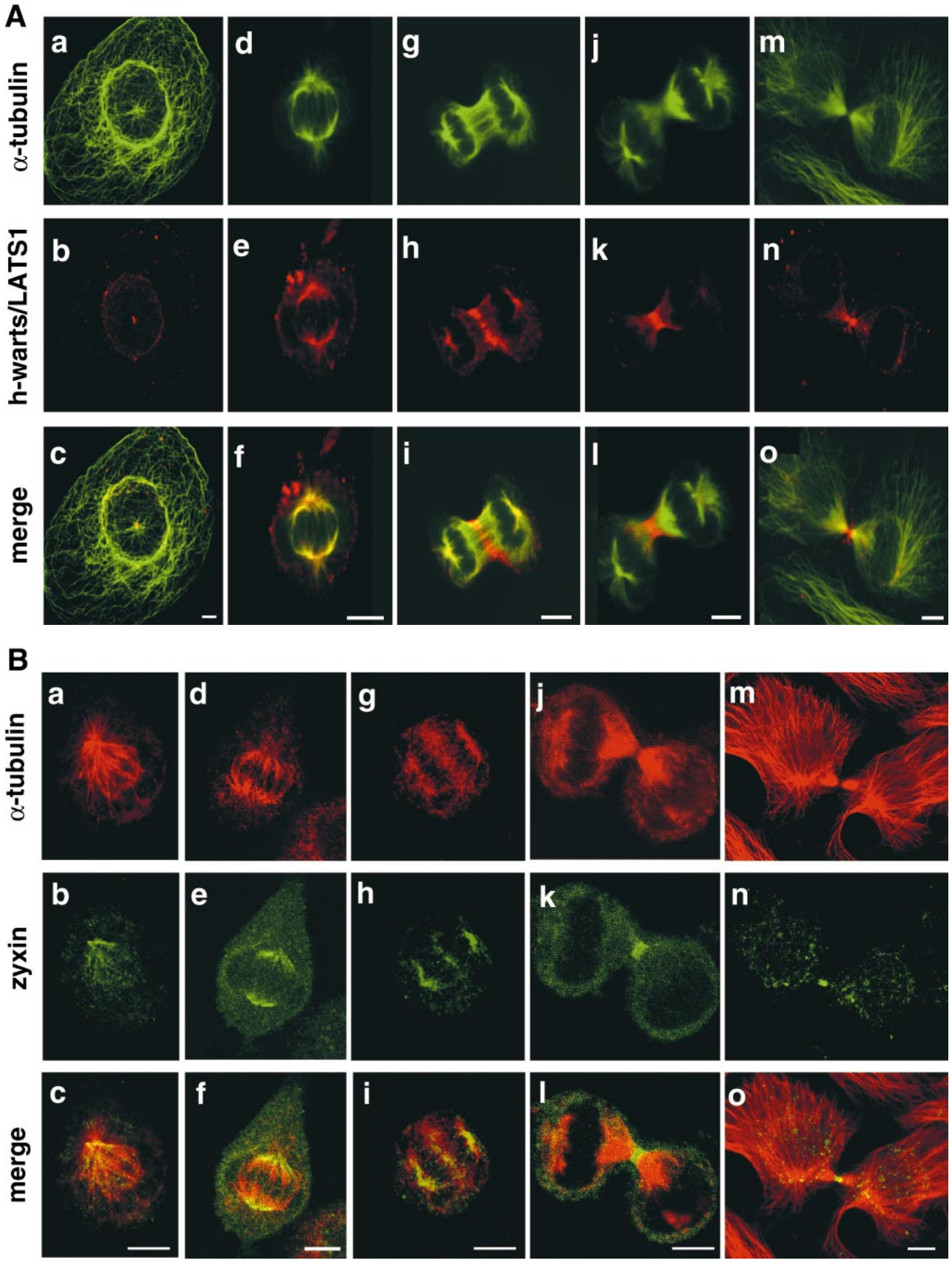

Figure 4 (continues on facing page).

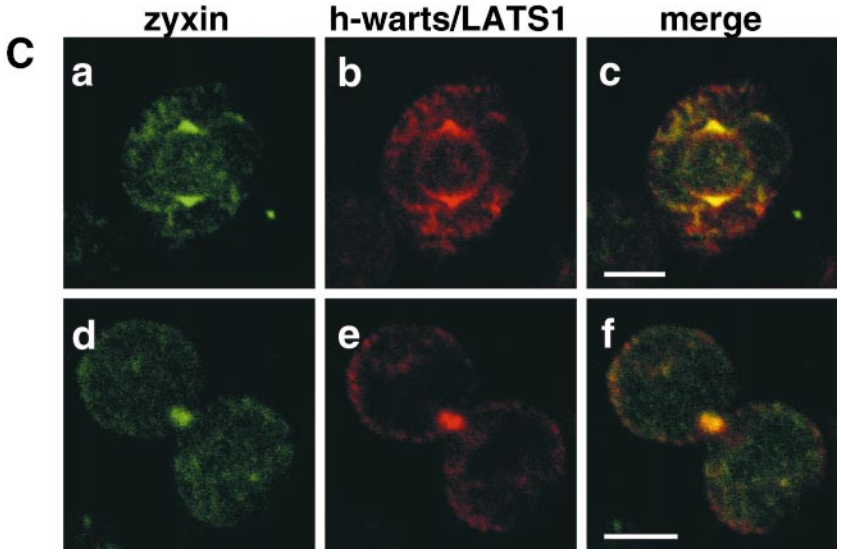

Figure 4. Colocalization of zyxin and h-warts/LATS1 to the mitotic apparatus. (A) Localization of h-warts/LATS1 at the different phases of the cell cycle. U2OS cells were preextracted with MSB (microtubule stabilizing buffer, including 0.5% Triton X-100) and fixed with cold methanol, followed by incubation with rat anti–h-warts antibody and mouse anti–α-tubulin antibody. Immunofluorescence staining was performed with FITC-conjugated anti–mouse IgG antibody (a, d, g, j and m) and Cy3-conjugated anti–rat IgG antibody (b, e, h, k, and n). The merged pictures of the upper two panels are shown in the lower panel (c, f, i, l, and o). Representative cells in interphase (a–c), metaphase (d–f), anaphase (g–i), telophase (j–l), and later telophase (m–o) are shown. (B) Distribution of zyxin during mitosis. U2OS cells were preextracted with 7.5 μg/ml digitonin/KHM, and fixed with cold methanol, after incubation with rabbit anti-zyxin antibody and mouse anti–α-tubulin antibody. Immunofluorescence staining was performed with Texas red–conjugated anti–mouse IgG antibody (a, d, g, j, and m) and FITC-conjugated anti–rabbit IgG antibody (b, e, h, k, and n). The merged pictures of the upper two panels are shown in the lower panel (c, f, i, l, and o). Representative cells in prometaphase (a–c), metaphase (d–f), anaphase (g–i), telophase (j–l), and later telophase (m–o) are shown. (C) Identical distribution of h-warts/LATS1 and zyxin to the mitotic apparatus. U2OS cells were prepared and fixed as in (A) and processed for incubation with rabbit anti-zyxin antibody (a and d) and rat anti–h-warts antibody (b and e). Immunofluorescence staining was performed with FITC-conjugated anti–rabbit antibody and Cy3-conjugated anti–rat IgG antibody. The merged pictures of the left two panels are shown in the right panel (c and f). Bars, 10 μm.

(Nishiyama et al., 1999; Tao et al., 1999) preferentially interacts with zyxin.

Zyxin Is Targeted to the Mitotic Apparatus by Interacting with h-warts/LATS1

To test whether dynamic changes in zyxin localization on the mitotic apparatus is dependent on h-warts/LATS1 distribution, we attempted to disrupt endogenous zyxin localization by injecting excessive amounts of an h-warts/LATS1 fragment (amino acids 136–700) that is shown to bind preferentially to zyxin (Fig. 2 B). Prophase/prometaphase U2OS cells were microinjected with purified GST–h-warts/LATS1(136–700) fusion protein, or control GST protein. Rhodamine-labeled tubulin was injected together with the GST fusion proteins not only to distinguish injected cells but to monitor mitotic spindle organization as the cell cycle proceeds. After injection, cells were subjected to the detergent-preextraction immunostaining with anti-zyxin antibody. Signal of endogenous zyxin on the mitotic apparatus was diminished or disappeared in 64% of the GST–h-warts/LATS1(136–700)–injected cells (n = 11), whereas it was decreased in only 18% of the GST-injected control cells (n = 12; Fig. 8). These observations indicate that association of zyxin with h-warts/LATS1 is essential for targeting as well as dynamic localization of zyxin on the mitotic apparatus during mitosis.

Biological Significance of h-warts/LATS1-Zyxin Complex on the Mitotic Apparatus

Since h-warts/LATS1 is speculated to be involved in mitotic control, the h-warts/LATS1-zyxin complex on the mitotic apparatus may play a role in proper execution of the mitotic process. To test this possibility, we examined whether h-warts/LATS1(136–700) microinjected cells can proceed through mitosis normally. HeLa cells, synchronized at S phase, were coinjected with GST–h-warts/LATS1 (136–700) or GST-mock and β-galactosidase to detect injected cells. Cells were fixed at various time points after release from an S phase block, and the frequency of mitotic cells (mitotic index) in cells having β-galactosidase activity was determined (Fig. 9 A). While the control experiments exhibited a peak mitotic index at 10.5 h after release from S phase and a decrease after 12 h, h-warts/LATS1(136–700)–injected cells revealed a high mitotic index after 10.5 h and continued to increase until 12 h after the release (Fig. 9 B). Apparently, cells injected with h-warts/LATS1(136–700) had a prolonged mitotic phase. These observations suggest that disruption of h-warts/LATS1-zyxin complex leads to impairment of normal mitotic progression.

Discussion

In searching for cellular targets of the h-warts/LATS1 tumor suppressor protein, we have identified zyxin which plays a central role in actin assembly and organization. During interphase, zyxin is found at cellular locations that are enriched in actin filaments, including the leading edge and focal adhesion plaques, whereas h-warts/LATS1 is localized to centrosome. However, during mitosis, when zyxin is dissociated from focal adhesions, a fraction of the free cytoplasmic zyxin becomes associated with mitotic spindles. We have shown that zyxin is phosphorylated during mitosis and that the mitotic phosphorylation is required for association with h-warts/LATS1 on the mitotic

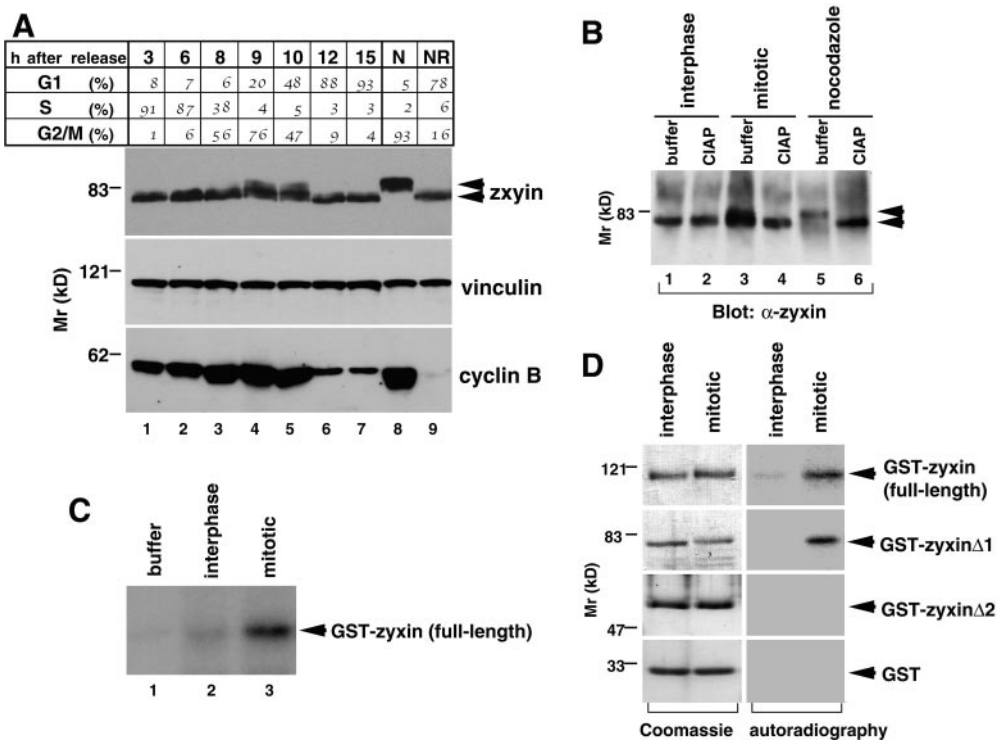

Figure 5. Mitosis-specific phosphorylation of zyxin. (A) Posttranslational modification of zyxin during the cell cycle. HeLa cells were synchronized at the beginning of S phase by the double thymidine block method. After release from S phase, cells were harvested at the indicated time points (lanes 1–7). To block cells at mitosis, nocodazole was added into the medium 6 h after release from S phase and incubated for another 6 h (N, lane 8). After removal of nocodazole, cells were incubated in nocodazole-free media for another 3 h to obtain interphase cells (NR, lane 9). Samples were analyzed for DNA content by flow cytometry. The percentages of the cells in G1, S, and G2/M are shown in the upper panel. Each sample was subjected to immunoblotting with anti-zyxin antibody, anti-vinculin antibody, and anti-cyclin B antibody. (B) Phosphatase treatment of zyxin. Endogenous zyxin was immunoprecipitated from interphase (lanes 1 and 2), mitotic (lanes 3 and 4) and nocodazole-treated (lanes 5 and 6) lysate and incubated with 100 units of calf intestine alkaline phosphatase (CIAP) (lanes 2, 4, and 6) or without CIAP (lanes 1, 3, and 5) at 37°C for 30 min. Equal amount of precipitants were immunoblotted with the anti-zyxin antibody. Arrows indicate the endogenous zyxin. (C) Detection of zyxin-kinase activity in mitotic cell lysate. GST-zyxin (full-length) was incubated in the presence of γ-[^{32}P]ATP with either buffer alone (lane 1), interphase cell lysate (lane 2), or mitotic cell lysate (lane 3) for 30 min at 25°C. GST-zyxin (full-length) was analyzed by SDS-PAGE and autoradiography. (D) Phosphorylation region of zyxin. Purified GST-zyxin, full-length and truncated mutants, as indicated (left; Coomassie blue staining), were subjected to in vitro kinase assay with interphase/mitotic cell lysate as described in (C) (right, autoradiography). Note that a fraction of protein was converted into the slow-mobility form after incubation with mitotic lysate in GST-zyxin (full-length) and zyxinΔ1.

apparatus. These findings implicate dual functions for zyxin: not only does it play a key role in cell adhesion and cytoskeletal organization in interphase cells, but it also acts as a participant in mitotic control by forming a complex with h-warts/LATS1 on the mitotic apparatus.

Regulation of the Interaction between h-warts/LATS1 and Zyxin

We have shown a physical association of zyxin with h-warts/LATS1 and that a region containing the first and second LIM domains (LIM1/2) of zyxin is responsible for the interaction. The LIM domain is a protein binding motif which is found in a wide variety of proteins involved in transcription, cell adhesion, and cytoskeletal organization (Schmeichel and Beckerle, 1994; Dawid et al., 1998). Proteins with multiple LIM domains, such as zyxin, are considered to function as scaffolds for the assembly of protein complexes. To date, only cysteine-rich protein 1 (CRP1) has been reported to associate with the LIM1 domain of zyxin (Sadler et al., 1992). Our findings demonstrated that a combination of LIM1 and LIM2 domains, but not that of LIM2 and LIM3, is essential for zyxin to interact with h-warts/LATS1, suggesting that a specific protein recognition mechanism is used for their interaction. The association of h-warts/LATS1 with the full-length zyxin has been detected by in vivo but not by in vitro binding experiments. However, the deletion of the NH_2-terminal region of zyxin has allowed the LIM1/2 domain to interact with h-warts/LATS1 in vitro. Therefore, we speculate that the LIM1/2 domains are masked in full-length zyxin and that the posttranslational modification, such as phosphorylation and/or proteolysis, gives rise to the conformational alterations in zyxin, exposing the LIM domains on the surface of the molecule, which allows h-warts/LATS1 to approach.

Although zyxin was first described as a phosphoprotein (Crawford and Beckerle, 1991), both the mechanism and the biological significance of the phosphorylation have remained elusive. In this study, we demonstrated that the NH_2-terminal region of zyxin is mitotically phosphorylated. Three lines of evidence presented here suggest that the mitotic phosphorylation of zyxin is mediated by Cdc2, a primary kinase to drive mitosis. First, depletion of Cdc2 from mitotic cell lysates completely abolished phosphorylation of zyxin. Second, purified active Cdc2 complex phosphorylated zyxin. Third, zyxin is phosphorylated during mitosis when Cdc2 is active. A number of studies have focused on the role of Cdc2 in the coordination of cellular and biochemical events during mitosis, and identification

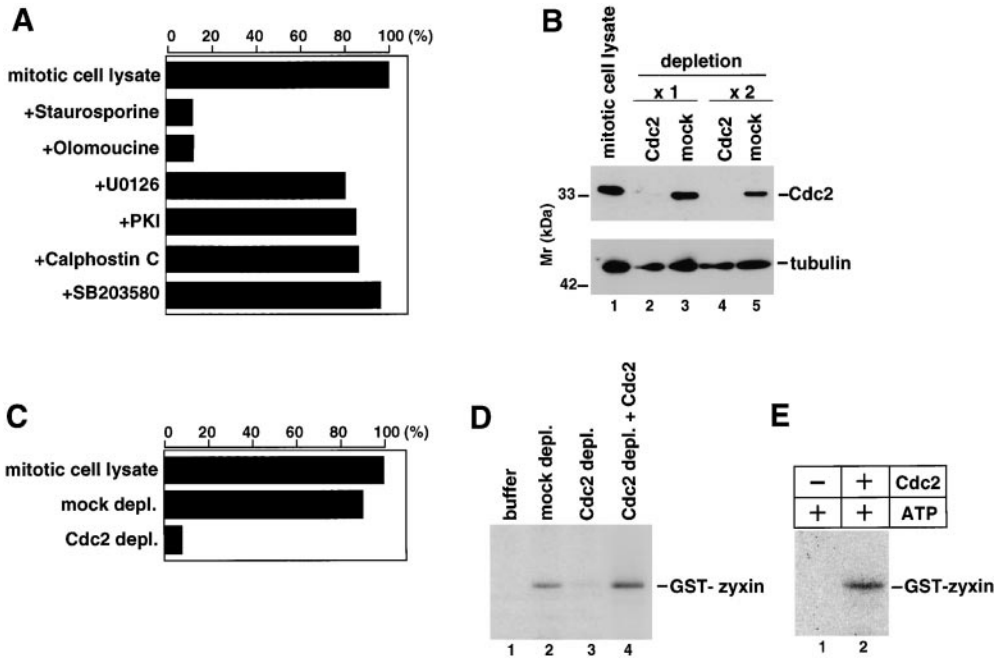

Figure 6. Characterization of zyxin-kinase. (A) Effect of protein kinase inhibitors on the zyxin-kinase activity in mitotic cell lysate. GST-zyxin (full-length) was incubated for 30 min at 25°C in the presence of γ-[^{32}P]ATP and mitotic cell lysate with the indicated protein kinase inhibitors as follows: 100 nM staurosporine (broad serine/threonine kinase inhibitor), 100 μM olomoucine (Cdc2 inhibitor), 100 μM U0126 (MEK1 inhibitor), 1 μM PKI (protein kinase A inhibitor), 100 nM calphostin C (protein kinase C inhibitor), 100 μM SB203580 (p38 kinase inhibitor), or without kinase inhibitor (mitotic cell lysate alone). Results are presented as the percentage of the levels of GST-zyxin phosphorylation, where 100% represents the phosphorylation level after incubation with mitotic cell lysate alone. (B) Depletion of Cdc2 from mitotic cell lysate. Mitotic cell lysate (lane 1) was incubated with p13-suc1–conjugated agarose beads to deplete Cdc2 (lanes 2 and 4). Mock depletion was performed by incubating the mitotic cell lysate with the same volume of unconjugated agarose beads (lanes 3 and 5). Unbound cytosolic proteins were immunoblotted with anti-Cdc2 (top) or anti–β-tubulin antibodies (bottom). (C) Histone H1 kinase activity of mitotic cell lysates. The peptide derived from histone H1 was incubated in the presence of γ-[^{32}P]ATP with mitotic cell lysate, mock-depleted lysate, or Cdc2-depleted lysate. Results are presented as percentage of the phosphorylation levels of the peptide, where 100% represents the phosphorylation level after incubation with the mitotic cell lysate. (D) Effect of Cdc2 depletion on the zyxin-kinase activity in mitotic cell lysate. GST-zyxin (full-length) was incubated in the presence of γ-[^{32}P]ATP with either buffer alone (lane 1), mock-depleted mitotic cell lysate (lane 2), or Cdc2-depleted mitotic cell lysate (lane 3), or Cdc2-depleted mitotic cell lysate supplemented with purified active Cdc2 complex (lane 4) for 30 min at 25°C. GST-zyxin (full-length) was analyzed by SDS-PAGE and autoradiography. (E) Direct phosphorylation of zyxin by Cdc2. GST-zyxin (full-length) was incubated in the presence of γ-[^{32}P]ATP with (lane 1) or without active Cdc2 complex (lane 2).

of its physiological substrates continues to represent a major challenge (Nigg et al., 1996; Nurse, 2000). It cannot be completely ruled out the possibility that another kinase phosphorylates zyxin in vivo. However, the previous findings that a fraction of the cellular pool of Cdc2 is associated with the mitotic spindle, where it forms an active kinase complex with cyclin B (Bailly et al., 1989), also supports our present observations.

As predicted by our hypothesis, the Cdc2-dependent phosphorylation has been shown to allow the full-length zyxin to interact with h-warts/LATS1 (Fig. 7 A). In fact, zyxin associates with h-warts/LATS1 preferentially during mitosis (Fig. 7 B), and this interaction might be significant for the subsequent cellular events in cell division. However, the binding of phosphorylated full-length zyxin to h-warts/LATS1 was not as efficient as that of the Δ2 protein (Fig. 7 A), so the possibility can not be excluded that the interaction is regulated by not only phosphorylation but other unknown modifications of full-length zyxin.

Spatial Control of Zyxin Localization during Mitosis

Zyxin has been shown to dissociate from focal adhesion plaques and to distribute diffusely into the cytoplasm coincidentally with the mitotic disappearance of focal adhesions. Subsequently, a fraction of this free cytoplasmic zyxin becomes colocalized with h-warts/LATS1 on the mitotic apparatus (Figs. 3 and 4). Since zyxin plays a critical role in the actin filament assembly at focal adhesions (Beckerle, 1998, 1997), dissociation of zyxin may contribute to actin stress fiber disassembly in the mitotic cells. The other focal adhesion components, such as paxillin (Yamaguchi et al., 1997) and p130CAS (Yamakita et al., 1999), have been reported to be phosphorylated during mitosis when focal adhesions dissociate. As for zyxin, it can be speculated that the mitotic phosphorylation is a signal for triggering detachment of zyxin from adhesion sites. However, two observations presented here support the possibility that mitotic phosphorylation is required mainly to recruit zyxin to the mitotic spindle. First, although most of the zyxin became dissociated during mitosis, both phosphorylated and dephosphorylated zyxin were detected in the cells at mitosis (Fig. 5, A and B). Second, the immunolocalization study demonstrated that a subfraction of zyxin localized to the mitotic apparatus (Fig. 3, C and D), which was clearly detected by the preextraction method (Fig. 4 B).

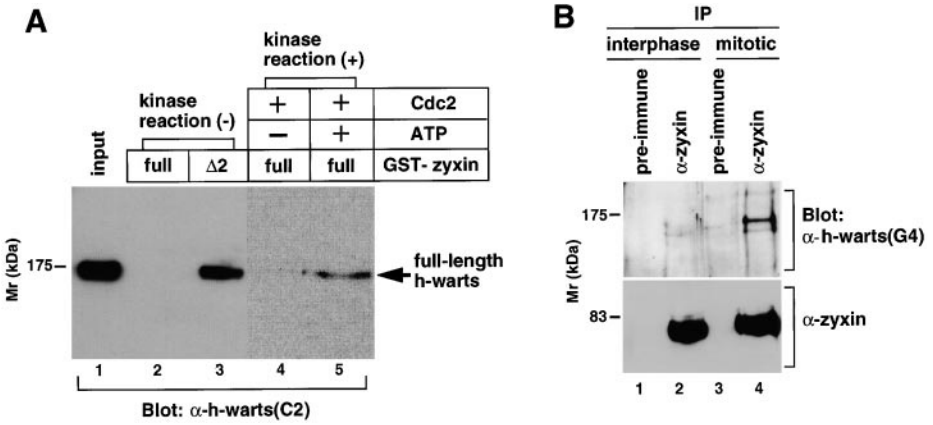

Figure 7. Regulation of h-warts/LATS1-zyxin association. (A) Association of h-warts/LATS1 with Cdc2-mediated phosphorylation of zyxin. 10 μg of GST-zyxin (full-length) was incubated with active Cdc2 complex with or without ATP for 30 min at 25°C as described in Fig. 6 E, followed by in vitro binding assay as in Fig. 2 C. After kinase reaction in the absence of ATP (lane 4), or in the presence of ATP (lane 5), GST-zyxin (full-length) were incubated with 1 μg of His-tagged h-warts/LATS1 (lane 1). Control experiments were performed without kinase reaction using GST-zyxin (full-length) (lane 2) or GST-zxyinΔ2 (lane 3). Bound fraction was analyzed by SDS-PAGE, followed by immunoblotting with the anti-C2 antibody. (B) Mitosis-specific interaction of h-warts/LATS1 and zyxin. The lysate of interphase (lanes 1 and 2) or mitotic (lanes 3 and 4) HeLa cells was immunoprecipitated with preimmune IgG (lanes 1 and 3) or with the anti-zyxin antibody (lanes 2 and 4). The immunoprecipitates were probed with anti–h-warts/LATS1 antibody (G4) or with anti-zyxin antibody as in Fig. 1 F.

Dynamic Interaction of h-warts/LATS1–Zyxin Protein Complex on the Mitotic Apparatus

The interaction between zyxin and h-warts/LATS1 on the mitotic apparatus implicates a significant role of actin regulatory proteins during mitosis. Zyxin serves as a scaffold for gathering actin regulatory proteins, such as Ena/VASP–profilactin complex or vav-small GTPase complex, at focal adhesion plaques (Beckerle, 1997). In fission yeast

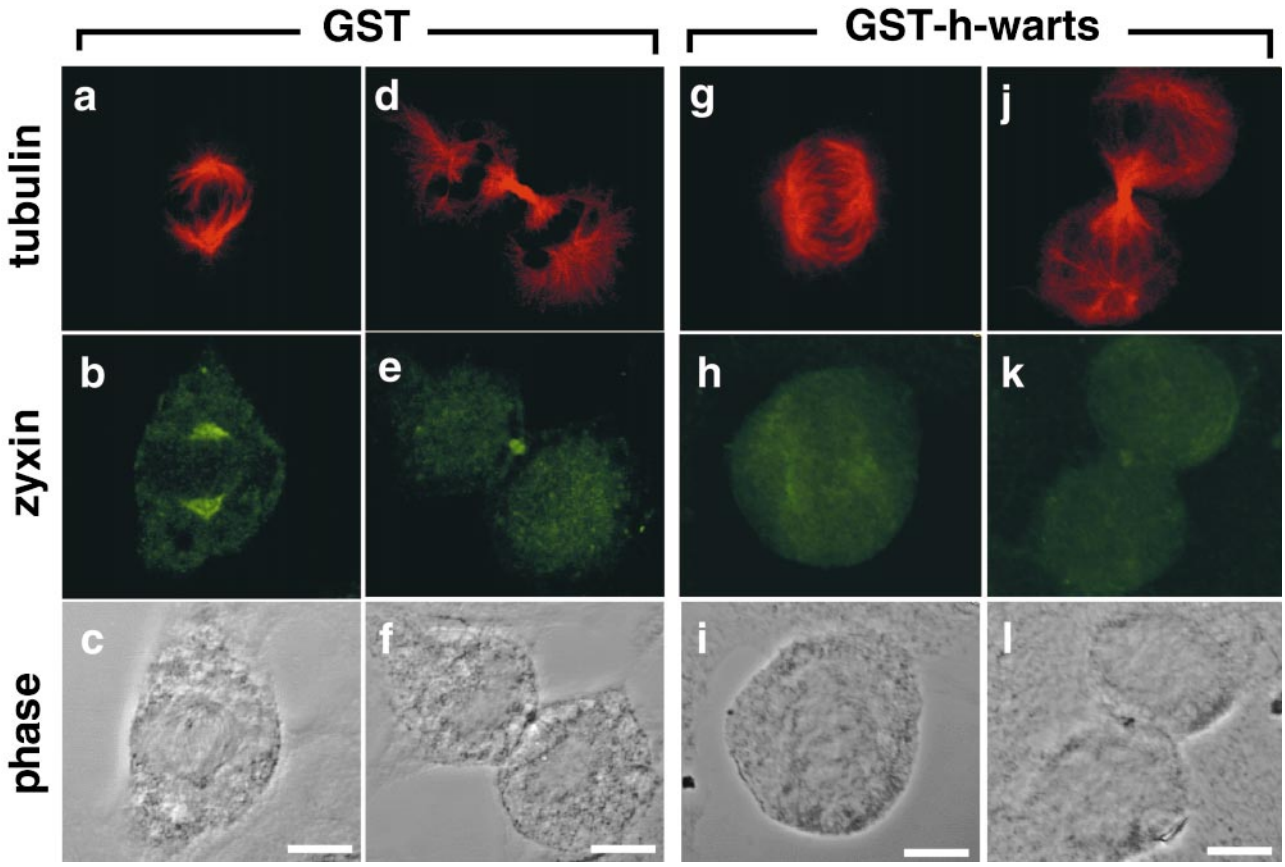

Figure 8. Disruption of endogenous zyxin localization on the mitotic apparatus by introducing h-warts/LATS1 protein fragments. U2OS cells were microinjected with 1.0 mg/ml of GST–h-warts/LATS1 (amino acids 135–700) or GST alone, supplemented with rhodamine-labeled tubulin. After preextraction and fixation, cells were incubated with rabbit anti-zyxin antibody and labeled with FITC-conjugated anti–rabbit IgG antibody. Cells with rhodamine-labeled mitotic spindles (a, d, g, and j) were evaluated for zyxin staining (b, e, h, and k). Representative pictures injected with GST alone (a–f), or GST–h-warts (amino acids 135–700; g–l) in metaphase and telophase are shown. The bottom panels (c, f, i, and l) show the phase-contrast images of the corresponding cells. Bars, 10 μm.

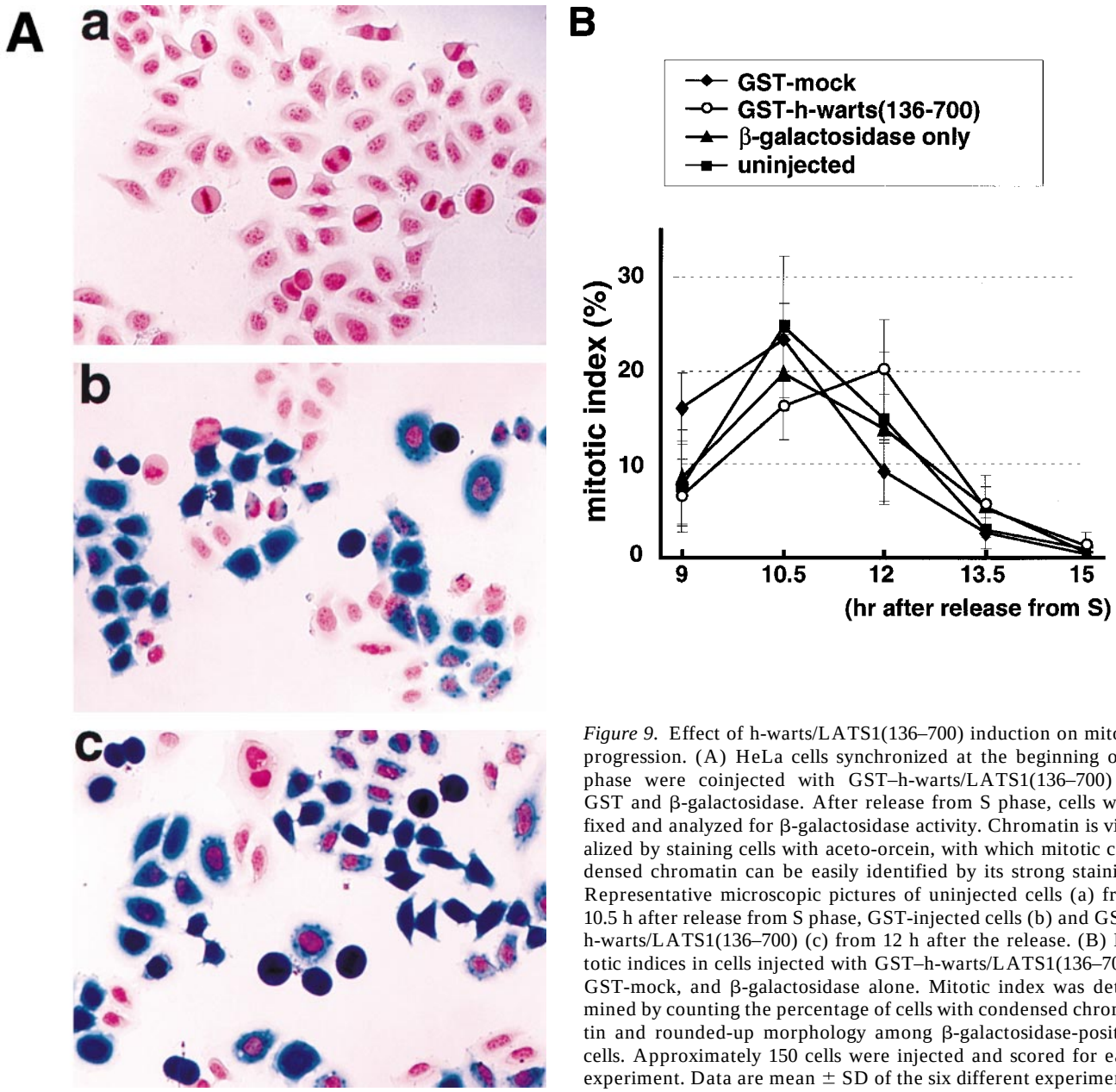

Figure 9. Effect of h-warts/LATS1(136–700) induction on mitosis progression. (A) HeLa cells synchronized at the beginning of S phase were coinjected with GST–h-warts/LATS1(136–700) or GST and β-galactosidase. After release from S phase, cells were fixed and analyzed for β-galactosidase activity. Chromatin is visualized by staining cells with aceto-orcein, with which mitotic condensed chromatin can be easily identified by its strong staining. Representative microscopic pictures of uninjected cells (a) from 10.5 h after release from S phase, GST-injected cells (b) and GST–h-warts/LATS1(136–700) (c) from 12 h after the release. (B) Mitotic indices in cells injected with GST–h-warts/LATS1(136–700), GST-mock, and β-galactosidase alone. Mitotic index was determined by counting the percentage of cells with condensed chromatin and rounded-up morphology among β-galactosidase-positive cells. Approximately 150 cells were injected and scored for each experiment. Data are mean ± SD of the six different experiments.

and *Drosophila*, defects in profilin, which is shown to be essential to form the actomyosin contractile ring, results in the failure of cytokinesis (Balasubramanian et al., 1994; Giansanti et al., 1998). Rho GTPase-mediated signal is required for the organization of cortical components to form the contractile ring in mammalian cells (O'Connell et al., 1999). Moreover, a number of genetic analyses converge on the idea that components associated with mitotic spindle may cooperate in formation of the contractile ring by mediating the biochemical signaling or the physical interaction between two structures (Williams et al., 1995; Adams et al., 1998). All these findings support the idea that zyxin also plays a role in cell division by regulating actin filament assembly at midzone of the dividing cell.

The duration of mitosis in cells injected with h-warts/LATS1(136–700) fragment, which significantly perturbed zyxin specifying to the mitotic apparatus, was significantly longer than that of control cells, mainly due to delay in exit from mitosis (Fig. 9). An intriguing explanation for the observation is that the mislocalization of zyxin, as well as zyxin-binding partners for actin polymerization, induces discoordination of contractile ring in dividing cells, and thereby delays their exit from mitosis. Alternatively, h-warts/LATS1 enzymatic activity may be modulated by zyxin, so that disruption of their interaction results in inactivation of h-warts/LATS1 itself. It can not be excluded, however, that another, as yet unknown, protein(s) is also functionally impaired by h-warts/LATS1(136–700) fragments to produce these results.

To maintain genomic stability and proper ploidy, it is crucial that cell division occurs at the end of anaphase after chromosome segregation. The molecular mechanism

through which h-warts/LATS1 serves as a tumor suppressor is unknown, but one possible explanation is that h-warts/LATS1 may play a critical role in cell division processes by forming a complex with zyxin on the mitotic apparatus. Abrogation of this interaction may involve failure in normal mitotic progression, leading to chromosomal instability, which is a hallmark of malignant tumors.

We thank Drs. Q. Hu, H. Maruta, and A. Kikuchi for providing the pCGN, pGEX2TH, and pBJ-Myc plasmids, respectively; Dr. K. Tanabe for critically reading the manuscript; Dr. J. Moon for editorial assistance; Drs. Y. Arima, S. Honda, M. Nitta, and H. Nakamura for valuable suggestions; Mr. K. Ida (Olympus) and Mr. K. Ueda (Uniscience) for technical assistance; and T. Arino for secretarial assistance.

This work was supported by a grant for Cancer Research from the Ministry of Education, Science and Culture of Japan (H. Saya).

Submitted: 16 November 1999
Revised: 14 April 2000
Accepted: 19 April 2000

References

Adams, R.R., A.A. Tavares, A. Salzberg, H.J. Bellen, and D.M. Glover. 1998. *pavarotti* encodes a kinesin-like protein required to organize the central spindle and contractile ring for cytokinesis. *Genes Dev*. 12:1483–1494.

Bahler, J., A.B. Steever, S. Wheatley, Y. Wang, J.R. Pringle, K.L. Gould, and D. McCollum. 1998. Role of polo kinase and Mid1p in determining the site of cell division in fission yeast. *J. Cell Biol*. 143:1603–1616.

Bailly, E., M. Doree, P. Nurse, and M. Bornens. 1989. p34cdc2 is located in both nucleus and cytoplasm; part is centrosomally associated at G2/M and enters vesicles at anaphase. *EMBO (Eur. Mol. Biol. Organ.) J.* 8:3985–3995.

Balasubramanian, M.K., B.R. Hirani, J.D. Burke, and K.L. Gould. 1994. The *Schizosaccharomyces pombe cdc3+* gene encodes a profilin essential for cytokinesis. *J. Cell Biol*. 125:1289–1301.

Beckerle, M.C. 1997. Zyxin: zinc fingers at sites of cell adhesion. *Bioessays*. 19: 949–957.

Beckerle, M.C. 1998. Spatial control of actin filament assembly: lessons from *Listeria*. *Cell*. 95:741–748.

Bischoff, J.R., and G.D. Plowman. 1999. The Aurora/Ipl1p kinase family: regulators of chromosome segregation and cytokinesis. *Trends Cell Biol*. 9:454–459.

Craig, S.W., and R.P. Johnson. 1996. Assembly of focal adhesions: progress, paradigms, and portents. *Curr. Opin. Cell Biol*. 8:74–85.

Crawford, A.W., and M.C. Beckerle. 1991. Purification and characterization of zyxin, an 82,000-dalton component of adherens junctions. *J. Biol. Chem*. 266: 5847–5853.

Crawford, A.W., J.W. Michelsen, and M.C. Beckerle. 1992. An interaction between zyxin and alpha-actinin. *J. Cell Biol*. 116:1381–1393.

Dawid, I.B., J.J. Breen, and R. Toyama. 1998. LIM domains: multiple roles as adapters and functional modifiers in protein interactions. *Trends Genet*. 14: 156–162.

Giansanti, M.G., S. Bonaccorsi, B. Williams, E.V. Williams, C. Santolamazza, M.L. Goldberg, and M. Gatti. 1998. Cooperative interactions between the central spindle and the contractile ring during *Drosophila* cytokinesis. *Genes Dev*. 12:396–410.

Glover, D.M., M.H. Leibowitz, D.A. McLean, and H. Parry. 1995. Mutations in aurora prevent centrosome separation leading to the formation of monopolar spindles. *Cell*. 81:95–105.

Golsteyn, R.M., K.E. Mundt, A.M. Fry, and E.A. Nigg. 1995. Cell cycle regulation of the activity and subcellular localization of Plk1, a human protein kinase implicated in mitotic spindle function. *J. Cell Biol*. 129:1617–1628.

Hobert, O., J.W. Schilling, M.C. Beckerle, A. Ullrich, and B. Jallal. 1996. SH3 domain-dependent interaction of the proto-oncogene product Vav with the focal contact protein zyxin. *Oncogene*. 12:1577–1581.

Izawa, I., N. Tamaki, and H. Saya. 1996. Phosphorylation of neurofibromatosis type 1 gene product (neurofibromin) by cAMP-dependent protein kinase. *FEBS Lett*. 382:53–59.

Jin, D.Y., F. Spencer, and K.T. Jeang. 1998. Human T cell leukemia virus type 1 oncoprotein Tax targets the human mitotic checkpoint protein MAD1. *Cell*. 93:81–91.

Justice, R.W., O. Zilian, D.F. Woods, M. Noll, and P.J. Bryant. 1995. The *Drosophila* tumor suppressor gene *warts* encodes a homolog of human myotonic dystrophy kinase and is required for the control of cell shape and proliferation. *Genes Dev*. 9:534–546.

Kimura, M., S. Kotani, T. Hattori, N. Sumi, T. Yoshioka, K. Todokoro, and Y. Okano. 1997. Cell cycle-dependent expression and spindle pole localization of a novel human protein kinase, Aik, related to Aurora of *Drosophila* and yeast Ipl1. *J. Biol. Chem*. 272:13766–13771.

Kusubata, M., T. Tokui, Y. Matsuoka, E. Okumura, K. Tachibana, S. Hisanaga, T. Kishimoto, H. Yasuda, M. Kamijo, Y. Ohba, et al. 1992. p13suc1 suppresses the catalytic function of p34cdc2 kinase for intermediate filament proteins, in vitro. *J. Biol. Chem*. 267:20937–20942.

Macalma, T., J. Otte, M.E. Hensler, S.M. Bockholt, H.A. Louis, M. Kalff-Suske, K.H. Grzeschik, D. von der Ahe, and M.C. Beckerle. 1996. Molecular characterization of human zyxin. *J. Biol. Chem*. 271:31470–31478.

Madaule, P., M. Eda, N. Watanabe, K. Fujisawa, T. Matsuoka, H. Bito, T. Ishizaki, and S. Narumiya. 1998. Role of citron kinase as a target of the small GTPase Rho in cytokinesis. *Nature*. 394:491–494.

Masuko, N., K. Makino, H. Kuwahara, K. Fukunaga, T. Sudo, N. Araki, H. Yamamoto, Y. Yamada, E. Miyamoto, and H. Saya. 1999. Interaction of NE-dlg/SAP102, a neuronal and endocrine tissue-specific membrane-associated guanylate kinase protein, with calmodulin and PSD-95/SAP90. A possible regulatory role in molecular clustering at synaptic sites. *J. Biol. Chem*. 274:5782–5790.

Nigg, E.A. 1998. Polo-like kinases: positive regulators of cell division from start to finish. *Curr. Opin. Cell Biol*. 10:776–783.

Nigg, E.A., A. Blangy, and H.A. Lane. 1996. Dynamic changes in nuclear architecture during mitosis: on the role of protein phosphorylation in spindle assembly and chromosome segregation. *Exp. Cell Res*. 229:174–180.

Nishiyama, Y., T. Hirota, T. Morisaki, T. Hara, T. Marumoto, S. Iida, K. Makino, H. Yamamoto, T. Hiraoka, N. Kitamura, and H. Saya. 1999. A human homolog of *Drosophila* warts tumor suppressor, h-warts, localized to mitotic apparatus and specifically phosphorylated during mitosis. *FEBS Lett*. 459:159–165.

Nix, D.A., and M.C. Beckerle. 1997. Nuclear-cytoplasmic shuttling of the focal contact protein, zyxin: a potential mechanism for communication between sites of cell adhesion and the nucleus. *J. Cell Biol*. 138:1139–1147.

Nurse, P. 2000. A long twentieth century of the cell cycle and beyond. *Cell*. 100: 71–78.

O'Connell, C.B., S.P. Wheatley, S. Ahmed, and Y.L. Wang. 1999. The small GTP-binding protein rho regulates cortical activities in cultured cells during division. *J. Cell Biol*. 144:305–313.

Prehoda, K.E., D.J. Lee, and W.A. Lim. 1999. Structure of the enabled/VASP homology 1 domain-peptide complex: a key component in the spatial control of actin assembly. *Cell*. 97:471–480.

Reinhard, M., K. Jouvenal, D. Tripier, and U. Walter. 1995. Identification, purification, and characterization of a zyxin-related protein that binds the focal adhesion and microfilament protein VASP (vasodilator-stimulated phosphoprotein). *Proc. Natl. Acad. Sci. USA*. 92:7956–7960.

Sadler, I., A.W. Crawford, J.W. Michelsen, and M.C. Beckerle. 1992. Zyxin and cCRP: two interactive LIM domain proteins associated with the cytoskeleton. *J. Cell Biol*. 119:1573–1587.

Schmeichel, K.L., and M.C. Beckerle. 1994. The LIM domain is a modular protein-binding interface. *Cell*. 79:211–219.

Sparks, C.A., M. Morphew, and D. McCollum. 1999. Sid2p, a spindle pole body kinase that regulates the onset of cytokinesis. *J. Cell Biol*. 146:777–790.

St. John, M.A., W. Tao, X. Fei, R. Fukumoto, M.L. Carcangiu, D.G. Brownstein, A.F. Parlow, J. McGrath, and T. Xu. 1999. Mice deficient of *Lats1* develop soft-tissue sarcomas, ovarian tumours and pituitary dysfunction. *Nat. Genet*. 21:182–186.

Sunkel, C.E., and D.M. Glover. 1988. polo, a mitotic mutant of *Drosophila* displaying abnormal spindle poles. *J. Cell Sci*. 89:25–38.

Tao, W., S. Zhang, G.S. Turenchalk, R.A. Stewart, M.A. St. John, W. Chen, and T. Xu. 1999. Human homologue of the *Drosophila melanogaster lats* tumour suppressor modulates CDC2 activity. *Nat. Genet*. 21:177–181.

Terada, Y., M. Tatsuka, F. Suzuki, Y. Yasuda, S. Fujita, and M. Otsu. 1998. AIM-1: a mammalian midbody-associated protein required for cytokinesis. *EMBO (Eur. Mol. Biol. Organ.) J.* 17:667–676.

Toyn, J.H., and L.H. Johnston. 1994. The Dbf2 and Dbf20 protein kinases of budding yeast are activated after the metaphase to anaphase cell cycle transition. *EMBO (Eur. Mol. Biol. Organ.) J.* 13:1103–1113.

Verde, F., D.J. Wiley, and P. Nurse. 1998. Fission yeast orb6, a ser/thr protein kinase related to mammalian rho kinase and myotonic dystrophy kinase, is required for maintenance of cell polarity and coordinates cell morphogenesis with the cell cycle. *Proc. Natl. Acad. Sci. USA*. 95:7526–7531.

Vojtek, A.B., S.M. Hollenberg, and J.A. Cooper. 1993. Mammalian Ras interacts directly with the serine/threonine kinase Raf. *Cell*. 74:205–214.

Williams, B.C., M.F. Riedy, E.V. Williams, M. Gatti, and M.L. Goldberg. 1995. The *Drosophila* kinesin-like protein KLP3A is a midbody component required for central spindle assembly and initiation of cytokinesis. *J. Cell Biol*. 129:709–723.

Xu, T., W. Wang, S. Zhang, R.A. Stewart, and W. Yu. 1995. Identifying tumor suppressors in genetic mosaics: the *Drosophila lats* gene encodes a putative protein kinase. *Development*. 121:1053–1063.

Yamaguchi, R., Y. Mazaki, K. Hirota, S. Hashimoto, and H. Sabe. 1997. Mitosis specific serine phosphorylation and downregulation of one of the focal adhesion protein, paxillin. *Oncogene*. 15:1753–1761.

Yamakita, Y., G. Totsukawa, S. Yamashiro, D. Fry, X. Zhang, S.K. Hanks, and F. Matsumura. 1999. Dissociation of FAK/p130(CAS)/c-Src complex during mitosis: role of mitosis-specific serine phosphorylation of FAK. *J. Cell Biol*. 144:315–324.

Yasui, Y., M. Amano, K. Nagata, N. Inagaki, H. Nakamura, H. Saya, K. Kaibuchi, and M. Inagaki. 1998. Roles of Rho-associated kinase in cytokinesis; mutations in Rho-associated kinase phosphorylation sites impair cytokinetic segregation of glial filaments. *J. Cell Biol*. 143:1249–1258.